PHYSICAL REVIEW B VOLUME 55, NUMBER 24 15 JUNE 1997-II

# Theoretical study of nonpolar surfaces of aluminum nitride: Zinc blende (110) and wurtzite $(10\bar{1}0)$

Ravindra Pandey and Peter Zapol
*Department of Physics, Michigan Technological University, Houghton, Michigan 49931*

Mauro Causà
*Dipartimento di Chimica Inorganica, Universita di Torino, 10125-Torino, Italy*

(Received 24 February 1997)

All-electron density-functional calculations are performed to study atomic structure and electronic properties of the nonpolar surfaces, namely zinc blende (110) and wurtzite $(10\bar{1}0)$ of AlN. Both surfaces are modeled using a two-dimensional periodic slab allowing the relaxation of the first two surface layers in the calculations. The results predict a small layer rotation angle accompanied by a contraction of Al-N bond length for both surfaces. These results do not follow the well-accepted *rotation-relaxation model* that predicts large layer rotation angles ($\sim 28°$) with no change in the bond length for most of the *III-V* semiconductor surfaces. Analysis of the relaxed configurations of the AlN surfaces in terms of atomic geometry, density of states, and charge density plots shows a presence of partial double-bond character in the surface Al-N bond. A similarity of these results with an earlier study on GaN nonpolar surfaces [J. E. Jaffe, R. Pandey, and P. Zapol, Phys. Rev. B **53**, R4209 (1996)] led us to suggest the *contraction-relaxation model* where the relaxation proceeds via strengthening of the surface bond. The primary driving force of such a type of relaxation appears to be the ability of nitrogen to form a double bond that facilitates redistribution of the charge density associated with anion dangling bond to the surface bond. [S0163-1829(97)52224-7]

Aluminum nitride is regarded as a wide band-gap semiconductor and is commonly used as a substrate for thin-film devices due to its high thermal conductivity and small thermal expansion coefficient. At ambient conditions, AlN crystallizes in the wurtzite phase although thin films of zinc-blende polytype were grown as well. For the bulk phase of AlN, recent theoretical calculations based on the Hartree-Fock[1,2] and density-functional methods[3–5] have obtained a very good description of its structural and electronic properties. However, such a detailed description of its surface properties is lacking. Previous theoretical studies[6–8] on AlN have considered the (110) zinc blende and $(10\bar{1}0)$ and $(11\bar{2}0)$ wurtzite surfaces yielding a totally different surface relaxations for these nonpolar surfaces. For the zinc-blende (110) surface, a surface layer rotation angle of about 21° was obtained[6] in contrast to a negative rotation angle of about 2.5° for the $(10\bar{1}0)$ wurtzite surface.[7] Based on the knowledge of physics and chemistry of tetrahedrally coordinated compounds occurring in both wurtzite and zinc-blende phases, one should not expect such a large difference in relaxation of the $(10\bar{1}0)$ and (110) surfaces of AlN. Furthermore, recent Hartree-Fock calculations on GaN $(10\bar{1}0)$ and (110) surfaces do indeed yield similar rotation angles of about 2°.[9] In this paper, we consider the $(10\bar{1}0)$ and (110) surfaces of AlN in the framework of density-functional theory with an aim to provide detailed and consistent results for surface relaxation. It is also expected that a complete understanding of the main cleavage planes of AlN would be helpful in further development of AlN-based thin-film devices.

Relaxed atomic geometry of the $(10\bar{1}0)$ and (110) surfaces is obtained by performing all-electron total-energy calculations using Perdew-Zunger parametrization[10] of the Ceperley-Alder results[11] for exchange and correlation functional in the local-density approximation. We employ a periodic approach for the calculations where the Bloch functions are constructed as linear combinations of atom-centered Gaussian orbitals. This method is implemented in the program package CRYSTAL and is described in detail elsewhere.[12,13] For integration in the reciprocal space, a grid of 24 $k$ points in the irreducible two-dimensional Brillouin Zone is used employing the method of Monkhorst and Pack.[14] Implementation of this method in the CRYSTAL program has been described by Pisani *et al.*[15,16]

For Al, the Gaussian basis set consists of four shells of $s$ type, three shells of $p$ type and two shells of $d$-type functions whereas the basis set for N consists of four shells of $s$ type and three shells of $p$ functions.[17] These basis sets reproduce bulk properties of AlN very well and include polarization functions for aluminum as suggested by earlier electronic structure calculations[1,2] to provide an adequate representation of the covalent bonding in the AlN lattice. The calculated lattice constant in the wurtzite phase is 3.099 Å with $c/a$ ratio of 1.61 as compared to the experimental value of 3.110 Å with $c/a$ ratio of 1.60.[18] For the zinc-blende phase, the calculated lattice constant is 4.345 Å.

We use the slab model to simulate the given surface, where the slab is made up of a finite number of neutral atomic layers. The slab is periodic in two dimensions with translational lattice constants that are $c$ and $a$ for the $(10\bar{1}0)$ wurtzite surface and $a$ and $a/\sqrt{2}$ for the (110) zinc-blende surface. For calculations, the thickness of the slab is generally chosen in such a way that first few surface layers are allowed to relax while the inner layers remain fixed to the

 

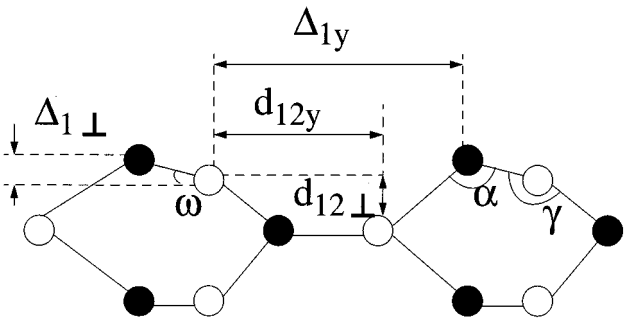


FIG. 1. A side view of atomic geometry of the first three layers of the AlN (110) surface. Open circles are Al atoms and filled circles are N atoms. Notations are the same as in Alves, Hebenstreit, and Scheffler (Ref. 20).

bulk geometry. In this paper, the slab simulating the $(10\bar{1}0)$ wurtzite surface consisted of six layers whereas the (110) zinc-blende surface is simulated by the five-layer slab model. In this way, relaxation is allowed for first two layers whereas the innermost layer is unrelaxed in both cases. Geometry optimization calculations begin with the ideal surface having atomic geometry of the bulk. The surface atoms associated with first and second layer are then allowed to relax until the change in total energy/unit cell is within approximately 1 meV. It leads to numerical uncertainty of about 0.02 Å in atomic displacements. Note that the slab is terminated on each side by the same surface and the symmetry is maintained throughout the optimization leading to the same surface relaxation on both sides of the slab.

We define the calculated structural parameters in Fig. 1 and summarize the results of surface geometry optimization in Table I. Here the layer rotation angle $\omega$ is defined as $\arctan(\Delta_{1,\perp}/(a-\Delta_{1,y})$ and the bond rotation angle $\theta$ is given by $\arctan(\Delta_{1,\perp}/\sqrt{(a-\Delta_{1,y})^2+\Delta_{1,x}^2})$. For the (110) surface, $\Delta_{1,x}=a/2\sqrt{2}$, while for the $(10\bar{1}0)$ surface $\Delta_{1,x}=0$. Therefore, $\omega$ and $\theta$ are distinct angles for the (110) surface, while they are equal angles for the $(10\bar{1}0)$ surface.

According to Table I, both surfaces exhibit similar relaxations that involve displacements of the surface Al and N atoms with respect to their ideal surface (bulk) configurations. This relative displacement of surface atoms yields the same bond rotation angle of 4.4° for the $(10\bar{1}0)$ and (110) surfaces, respectively. The layer rotation angle for the zinc-blende surface comes out to be 8.8°. Both surfaces have similar values for the surface buckling ($\Delta_{1,\perp}$) and in-plane spacing ($\Delta_{1,y}$ and $d_{12,y}$). The second-layer relaxation parameters (e.g., second-layer buckling) are found to very small. For the surface bond length, the calculated values show a contraction of about 6% with respect to the bulk bond length of 1.88 Å. A smaller contraction occurs for the back bond lengths in both surfaces. For example, the calculated values of the back bond lengths are 1.85 and 1.86 Å for the Al and N atoms, respectively, as compared to the bulk value of 1.88 Å for the (110) surface.

TABLE I. Calculated structural parameters for the relaxed AlN surfaces.

| Property | Wurtzite $(10\bar{1}0)$ | Zinc blende (110) |
|---|---|---|
| Bulk lattice constants, Å | | |
| $c$ | 5.002 | |
| $a$ | 3.099 | 4.345 |
| Displacements, Å | | |
| $\Delta_{1,\perp}$ | 0.14 | 0.14 |
| $d_{12,\perp}$ | 0.60 | 1.35 |
| $\Delta_{1,y}$ | 3.23 | 3.47 |
| $d_{12,y}$ | 2.61 | 2.35 |
| Rotational angles, ° | | |
| $\omega$ (layer) | 4.4 | 8.8 |
| $\theta$ (bond) | 4.4 | 4.4 |
| Bond lengths | | |
| $R$(Al-N), Å | 1.78 | 1.77 |
| $\Delta R$(Al-N) | −5.8% | −5.7% |

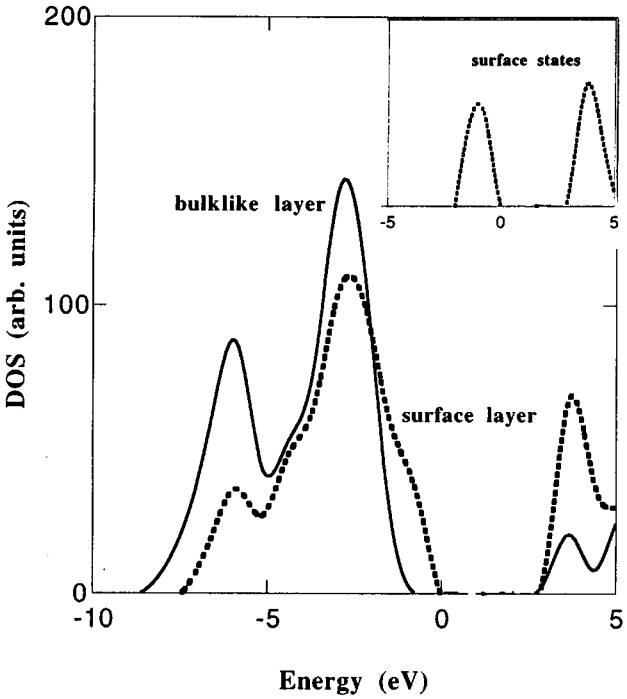


FIG. 2. (a) Projected density of states (PDOS) of the bulklike and surface layers of the AlN (110) surface. (b) The inset shows the surface states obtained by subtracting PDOS of the bulklike layer from the PDOS of the surface layer.

The difference in total energies of the relaxed and ideal surface configurations is defined as the relaxation energy. For the $(10\bar{1}0)$ and (110) surfaces, the relaxation energy per surface unit cell is calculated to be 0.54 and 0.47 eV, respectively. The surface energy is defined as $S=(n\times E_{\text{bulk}}-E_{n-\text{layer slab}})/2$, where $n$ is the number of layers in the slab simulating the surface. The surface energy per formula unit comes out to be 2.79 and 2.61 eV for the $(10\bar{1}0)$ and (110) surfaces, respectively. These surface energies are relatively higher than those reported for most of the other III-V semiconductors and are representative of a stronger Al-N bond in the lattice. We notice here that the cohesive energy of AlN is reported[2] to be 11.6 eV, giving the Al-N bond energy of 2.9 eV, since there are four bonds per Al-N pair in the lattice.

Figure 2 shows density of states projected on to a set of atomic orbital (PDOS) associated with atoms of the bulklike

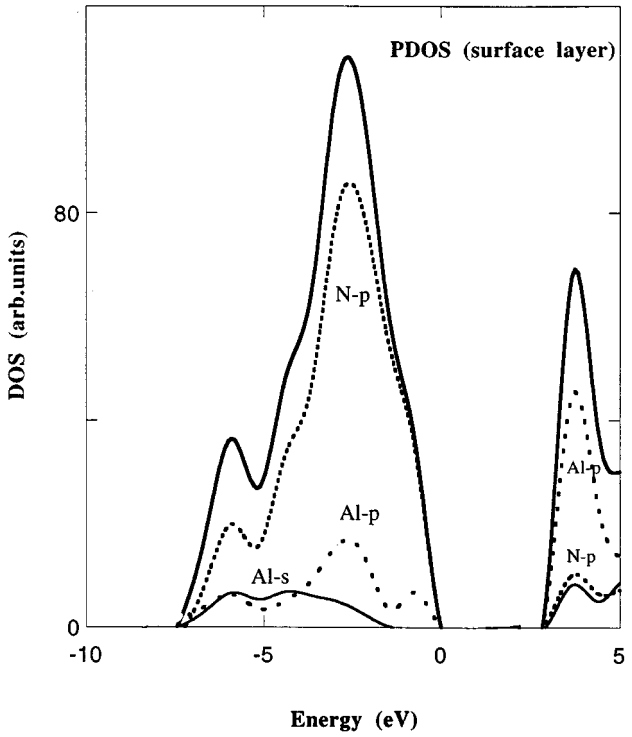


FIG. 3. Projected density of states for the surface layer of AlN (110) surface.

(innermost) and surface (outermost) layers of the (110) slab. The appearance of surface states in the fundamental gap is illustrated in Fig. 2(b), where we subtract contributions of the bulk PDOS from surface PDOS. Although, the occupied and unoccupied surface states are localized on the N and Al atoms, respectively, both states have substantial mixing of the Al and N orbitals as shown in Fig. 3.

Surface relaxation of the (110) surface is generally described by the rotation-relaxation model in which displacement of surface atoms occurs without the change in their bond lengths. It is now well established that such displacements yield a large value of layer rotation angle ($\sim 28°$) for most of the III-V semiconductors including AlP and GaAs.[19,20] In contrast to this well-accepted model, our results for AlN do not show such relaxation, yielding a small layer rotation angle of about 9° with a large contraction of about 6% in the bond length. A similar relaxation of surface atoms, i.e., small bond rotation angle with large bond contraction, has been found for the (110) and $(10\bar{1}0)$ surfaces of GaN.[9,21] Our results disagree with earlier calculations[6,7] that reported the rotation angle of 21° and $-2.5°$ for the (110) and $(10\bar{1}0)$ surfaces, respectively. We believe that the results of these calculations are not expected to be reliable due to use of either a four-atom cluster to simulate the (110) surface[6] or the rigid-rotation model that does not allow the change in bond length during relaxation of the $(10\bar{1}0)$ surface.[7]

Based on the local valence considerations, atoms on the relaxed surface of the III-V semiconductors are expected to mimic their configuration to that of their respective trihydrides.[6,22] Accordingly, the relaxed AlN surface configurations should result in a pyramidal angle $\alpha$ (at N) of 106.5° as in $NH_3$, and a planar angle $\gamma$ (at Al) of 120° as in

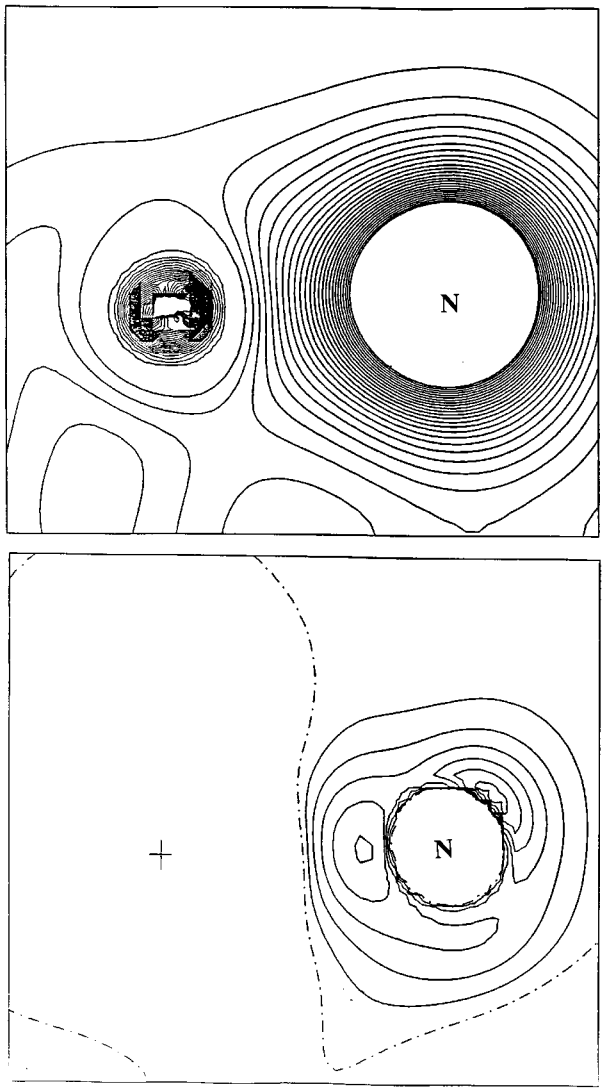


FIG. 4. Total and differential charge density maps of the AlN (110) relaxed surface that are projected on a plane perpendicular to the [110] direction. The differential map is obtained by subtracting the contributions of the Al and N atomic charge density from the total charge density. Solid and dashed lines indicate positive and negative difference values, respectively. The electron density spacing is 0.1 and 0.01 e/bohr$^3$ for total and differential maps, respectively. Atomic cores are not shown in the total charge density map.

$AlH_3$. For the ideal surface, $\alpha$ and $\gamma$ have the values of 109.47°, represents the tetrahedral coordination of atoms. The relaxed configuration, however, yields the bond angles 113.4° and 113.2° for $\alpha$ and $\gamma$, respectively (Fig. 1). This is due to the fact that atoms on the relaxed surface show smaller displacements parallel to the surface normal as compared to displacements expected solely from the local valence picture. The calculated results therefore suggest that the Al and N atoms on the relaxed (110) surface do not have bonding environment that is expected from their respective trihydrides.

We now focus on the electron charge density maps (Fig. 4) to investigate further the cause of this unusual relaxation of the AlN surfaces. Figure 4 shows total and differential charge density maps for the (110) surface where a build up of charge density along the Al-N bond length on the surface

is clearly visible. This figure also shows the charge density associated with the dangling bond lobe at the N site. The differential map is obtained by subtracting the contributions of the Al and N atomic charge density from the total charge density. Comparison with a charge density map for the ideal surface (not shown in Fig. 4) indicates the occurrence of charge transfer from the N dangling bond lobe to surface bond region upon relaxation. Mulliken population analysis also confirms this charge transfer showing a significant increase in the overlap population of the surface Al-N bond upon relaxation. For the ideal surface, the overlap population is $0.17e$ whereas the relaxed surface configuration shows the overlap population of $0.30e$ for the surface bond.

In an earlier study on GaN,[9] we have obtained similar results for relaxations of the (110) surface and have proposed that small surface rotation angles may be due to either hybridization effects of Ga-*d* states with N-*s* states in the valence band or the ability of N atoms to form double bonds. For AlN, we can easily rule out the *d*-*s* hybridization effects on the surface relaxation as aluminum does not have any occupied *d* orbitals. On the other hand, the calculated results for the relaxed configurations [i.e., a build up of charge density in the surface bond region and a mixed N($p$)-Al($p$) character of surface states] strongly indicate towards a partial double-bond character of the surface Al-N bond. The shortening of the surface bond length upon relaxation further supports the presence of a double bond that makes the Al-N bond relatively stronger at the surface.

In summary, we have studied atomic structure and electronic properties of the nonpolar surfaces of AlN. The calculated results predict small layer rotation angle accompanied by contraction of the Al-N bond length for the (110) and $(10\bar{1}0)$ relaxed surfaces. We explain the calculated results in the framework of the contraction-relaxation model, where redistribution of the charge density (associated with anion dangling bond) to the surface bond appears to be the driving force for the surface relaxation. It leads to the large contraction ($\sim 6\%$) of the surface bond. This is in contrast to the rotation-relaxation model where redistribution of the charge density occurs to the back leading to no change in the surface bond length upon relaxation.

The authors thank John Jaffe for helpful discussions. This work was supported by the Air Force Office of Scientific Research under Grant No. F49620-96-1-0319.

[1] R. Pandey, A. Sutijianto, M. Seel, and J. E. Jaffe, J. Mater. Res. **8**, 1922 (1993).
[2] E. Ruiz, S. Alvarez, and P. Alemany, Phys. Rev. B **49**, 7115 (1994).
[3] P. E. VanCamp, V. E. VanDoren, and J. T. Devreese, Phys. Rev. B **44**, 9056 (1991).
[4] N. E. Christensen and I. Gorczyca, Phys. Rev. B **47**, 4307 (1993).
[5] K. Kim, W. R. L. Lambrecht, and B. Segall, Phys. Rev. B **53**, 16 310 (1996).
[6] C. A. Swarts, W. A. Goddard, and T. C. McGill, J. Vac. Sci. Technol. **17**, 982 (1980).
[7] M. H. Tsai, R. V. Kasowski, and J. D. Dow, Solid State Commun. **64**, 231 (1987).
[8] K. Kadas, S. Alvarez, E. Ruiz, and P. Alemany, Phys. Rev. B **53**, 4993 (1996).
[9] J. E. Jaffe, R. Pandey, and P. Zapol, Phys. Rev. B **53**, R4209 (1996).
[10] J. P. Perdew and A. Zunger, Phys. Rev. B **23**, 5048 (1981).
[11] D. M. Ceperley and B. J. Alder, Phys. Rev. Lett. **45**, 566 (1980).
[12] M. Towler, A. Zupan, and M. Causà, Comput. Phys. Commun. **98**, 181 (1996).
[13] R. Dovesi, V. R. Saunders, C. Roetti, M. Causà, R. Orlando, N. M. Harrison, and E. Apra, CRYSTAL96, User Documentation, 1996, University of Torino and Daresbury Laboratory.
[14] H. J. Monkhorst and J. D. Pack, Phys. Rev. B **13**, 5118 (1976).
[15] C. Pisani, E. Aprà, and M. Causà, Int. J. Quantum Chem. **38**, 395 (1990).
[16] C. Pisani, E. Aprà, M. Causà, and R. Orlando, Int. J. Quantum Chem. **38**, 415 (1990).
[17] Basis sets can be obtained from the authors.
[18] H. Schulz and K. H. Thiemann, Solid State Commun. **23**, 815 (1977).
[19] J. P. LaFemina, Surf. Sci. Rep. **16**, 133 (1992).
[20] J. L. A. Alves, J. Hebenstreit, and M. Scheffler, Phys. Rev. B **44**, 6188 (1991).
[21] J. E. Northrup and J. Neugebauer, Phys. Rev. B **53**, R10 477 (1996).
[22] C. A. Swarts, T. C. McGill, and W. A. Goddard, Surf. Sci. **110**, 400 (1981).